

Broadband Epsilon Negative Transmission Line Resonant Antenna with AIS Loading

Liang-Yuan Liu^{1, 2, *} and Bing-Zhong Wang¹

Abstract—A metamaterial-based broadband antenna loaded with artificial impedance surface (AIS) is presented in this letter. Two metallic vias connect a Y-shaped patch to the ground plane. The patch, two metallic vias, and the AIS compose an epsilon negative (ENG) transmission line (TL). The asymmetry Y-shaped patch and the AIS bring about the first-order resonance (FOR) and second-order resonance (SOR) modes, which can be merged into one passband to yield a wideband property. The proposed ENG-TL resonant antenna has the advantages of compact size, wide bandwidth, and high gain, which can be applied to portable and handheld communication system.

1. INTRODUCTION

Metamaterials have been widely studied for antenna design. The metamaterial-based antennas improve the radiation properties of the antennas, such as bandwidth, gain, and efficiency. Metamaterial is used as antenna substrate to enhance gain [1]. Based on the left-handed property of the metamaterial with negative phase constant and zero propagation constant, metamaterial transmission line (TL) can be used to design miniaturized antennas and other microwave devices. One of its applications is the zeroth-order resonance (ZOR) antennas [2]. Although left-handed antennas offer an alternative solution for multiband operation with size miniaturization, they suffer from narrow bandwidth [3]. Many researchers have attempted to extend the bandwidth of the metamaterial-based antenna. The modified split-ring resonator structure with capacitively loaded strips result in a wide bandwidth [4]. In reference [5], by using the dual resonant modes, the fractional bandwidth is increased up to 25%. With the aid of reactive loading, a multiband metamaterial monopole antenna is proposed in [6]. A dual mode wideband ZOR and positive order resonance (POR) antenna loading with metamaterial for wideband application is presented in [7]. The metamaterial antenna excites ZOR and FOR modes for the bandwidth enhancement, decreases resonant frequencies, and enhances bandwidth [8]. The ZOR and first-order resonance (FOR) modes can be merged into one single band, and the bandwidth of the epsilon negative (ENG) antenna is extended up to 67.4% [9].

Artificial impedance surface (AIS) is a kind of resonant type microwave photonic crystals. The AIS can be utilized to miniaturize antenna size, enhance antenna bandwidth, and improve antenna radiation performance [10]. In [11], a multi-band and dual-mode antenna employing left-handed structures is developed, which can suppress the surface wave and improve front to back ratio. The mushroom-like metamaterial structure loaded with the reactive impedance surface (RIS) achieves the miniaturization of the antenna. A narrow band RIS antenna loaded with complementary split-ring resonators (CSRRs) is proposed [12]. By etching the highly anisotropic slot on the RIS, the antenna's miniaturization has been successfully fulfilled [13]. Although the metamaterial antennas loaded with RIS provide the advantage of size reduction, they suffer from narrow bandwidth [10–13].

Received 27 February 2016, Accepted 18 April 2016, Scheduled 27 April 2016

* Corresponding author: Liang-Yuan Liu (liuly1997@126.com).

¹ Institute of Applied Physics, University of Electronic Science and Technology of China, Chengdu, Sichuan, China. ² Department of Physics and Information Engineering, Huaihua University, Huaihua, Hunan, China.

This letter presents the theoretical modeling and analysis of an ENG-TL antenna composed of two-dimensional AIS metamaterial. The AIS is a periodic array of metallic unit cells printed on a dielectric substrate. A Y-shaped patch connects the AIS through two metallic via holes. By optimizing its configuration and size, the antenna can be compact in a very wide frequency band. Unlike the ZOR and FOR antennas in previous literatures, in this letter, the research focus shifts to merge the FOR and the SOR into one passband. The broadband antenna with a small size is designed and optimized.

2. ANTENNA THEORY

The antenna's substrate affects its radiation and input impedance characteristic. The AIS with reactive impedance observably reduces electromagnetic mutual coupling between the radiating element and ground plane. For a metamaterial antenna loaded with AIS, the image current is not parallel and symmetric to the original current distribution. The AIS loaded with a short-circuited transmission line does not support propagating surface waves. The magnetic energy stored in the AIS compensates for the electric energy stored in near field of the source itself. The dielectric substrate and the AIS constitute a novel artificial impedance substrate. The novel substrate can reduce adverse effects of the source itself and its image, which can realize a broadband impedance matching.

Figure 1(a) shows the resonant circuit model of the ENG-TL antenna, and Fig. 1(b) shows the simplified equivalent circuit model of the ENG TL. A traditional antenna is composed of right-handed series inductance and shunt capacitance. Two vias connecting the ground plane and the AIS structure can provide the left-handed effect. The fundamental ENG TL is composed of the left-handed inductance L_L of the metamaterial structure and the right-handed inductance L_R (capacitance C_R) of a conventional antenna. The inductance and capacitance of the ENG-TL antenna are subtly combined so that a relatively low frequency can be achieved.

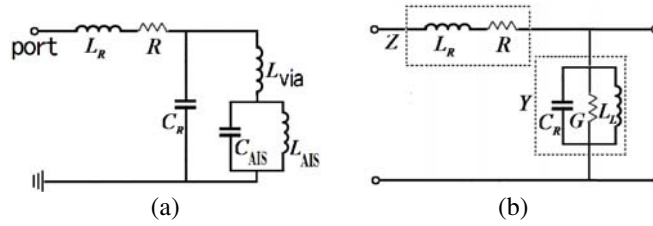


Figure 1. Equivalent circuit model for (a) the ENG-TL antenna, (b) the ENG TL.

The ENG TL has negative permittivity property in the special frequency band, which can excite both backward wave and forward wave at the same time. The ENG TL with both left-handed and right-handed properties simultaneously supports a specific positive phase constant and negative phase constant. As a result, an infinite wavelength wave at the boundary of passband and stop band of non-zero frequency achieves. The ENG-TL structure results in a sub wavelength resonance when the input admittances are determined by

$$Y_{inL} = Y_{inR} \quad (1)$$

where the left-handed input admittance $Y_{inL} = j \tan(\beta_L d_L) / Z_{0L}$, the right-handed input admittance $Y_{inR} = j \tan(\beta_R d_R) / Z_{0R}$. d_L is the length of left-handed transmission line, d_R the length of right-handed transmission line, Z_{0L} the characteristic impedance of left-handed transmission line, Z_{0R} the characteristic impedance of right-handed transmission line, and β the phase constant of electromagnetic wave.

According to the lossless transmission line theory, from the equivalent circuit model of the ENG-TL [14], the dispersion relation can be decided as

$$\cos(\beta \Delta x) = 1 - \frac{1}{2} L_R C_R \left(\omega^2 - \frac{1}{L_L C_R} \right) \quad (2)$$

where Δx is the length of the transmission line. When $\beta = 0$, an infinite wavelength can be supported, and a miniaturized resonant cavity can be achieved.

$$\beta = n\pi/l, \quad n = 0, \pm 1, \dots, \pm(N-1) \quad (3)$$

where l and N are total physical length of the resonator and numbers of resonator cells. When the mode numbers $n = 0$, the phase constant of the ENG TL is zero at non-zero frequency, other than the conventional half-wavelength resonance. A compact ZOR antenna can be implemented.

According to the open-ended boundary condition, the input impedance can be obtained as [15]

$$Z_{in} = -jZ_0 \cot \beta l = \frac{1}{N(j\omega C_R + 1/j\omega L_L)} \tag{4}$$

Equation (4) shows that the left-handed inductance L_L and the right-handed capacitance C_R determine the impedance characteristic. The subtle combination of L_L and C_R achieve a desired broadband impedance matching.

3. ANTENNA DESIGN

According to the aforementioned analysis, an ENG-TL antenna by loading the AIS is designed. As shown in Fig. 2, the AIS consists of a array of 8×6 square metallic unit cells, which is printed on the bottom of a dielectric substrate with a relative permittivity of 2.65, thickness of 1.5 mm, and loss tangent $\tan \delta = 0.002$. The dimension of the metallic unit cell is much smaller than the resonant wavelength. Two metallic shorting vias connect the Y-shaped patch and the AIS. The feed line at the center is employed to match the ENG-TL antenna with a 50Ω coaxial cable. In order to improve the impedance matching of the antenna, the width and length of the microstrip transmission line are optimized. The Y-shaped patch and two vias provide a means of controlling the equivalent circuit parameters very expediently.

To investigate the performance of the ENG-TL antenna, a prototype has been fabricated, and its photograph is shown in Fig. 3. The main dimensions are listed in Table 1.

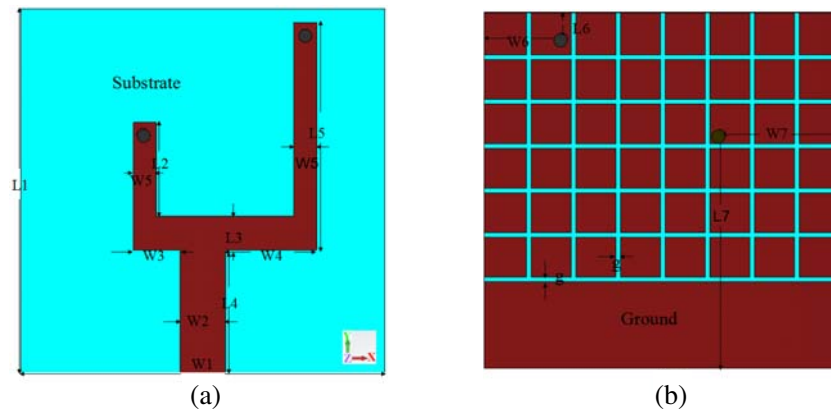


Figure 2. Configuration of antenna. (a) Top view. (b) Bottom view.

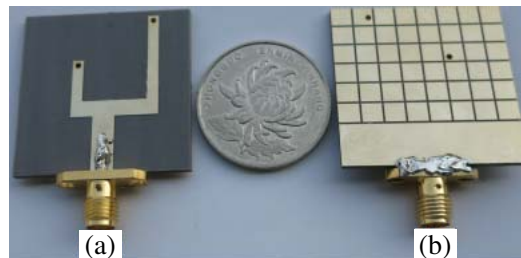


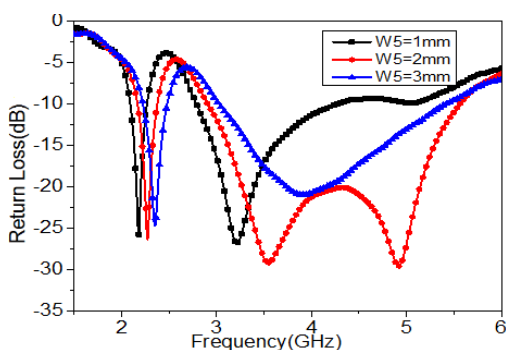
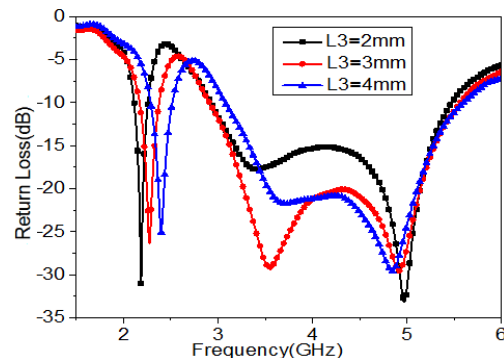
Figure 3. Photograph of the fabricated antenna. (a) Top view. (b) Bottom view.

Table 1. Dimensions of the proposed antenna. (UNIT: mm).

W_1	W_2	W_3	W_4	W_5	W_6	W_7	g
32	4	4.1	8	2	7.1	10.9	0.4
L_1	L_2	L_3	L_4	L_5	L_6	L_7	
32	8.2	3	10.8	20	3.2	21	

4. SIMULATION AND EXPERIMENTAL RESULTS

Compared to the conventional patch antenna with a perfectly electric conductor ground plane, the quality factor of the ENG-TL antenna decreases. Due to the asymmetric Y-shaped structure, higher-order resonance can be excited. In order to achieve a broadband performance and keep high efficiency, the ZOR, FOR and SOR are excited at the same time. Moreover, the FOR and SOR are merged into one passband. The ENG-TL antenna keeps the design freedom by controlling reactance and capacitance of the equivalent circuit. To verify the proposed design, the broadband ENG-TL antenna has been simulated using the time domain solver in CST Microwave Studio.

**Figure 4.** Simulated return loss of the proposed antenna with different widths of Y-shaped patch.**Figure 5.** Simulated return loss of the proposed antenna with different lengths L_3 .

The effects of the width of Y-shaped patch on return loss are depicted in Fig. 4. From studying these data, for the width of Y-shaped patch $W_5 = 2$ mm, the FOR and SOR are merged into one broad band. A fine control on working frequency with broadband impedance matching is achieved.

In Fig. 5. The Y-shaped patch with three different lengths L_3 , is analyzed as other parameters are fixed. The down band is affected slightly when the length L_3 varies from 2.0 mm to 4.0 mm in steps of 1.0 mm. However, the upper band is strongly dependent on L_3 . For $L_3 = 3$ mm, the FOR and SOR can be excited to form a wide impedance bandwidth.

The effects of the metallic shorting vias are analyzed in Fig. 6. Due to the change of surface current path, it is found that the widest impedance bandwidth is obtained for two metallic shorting vias. It can be seen that the frequency band undergoes a blue shift without via observably.

The simulated and measured return loss characteristics of the proposed antenna are plotted in Fig. 7. It can be observed that the simulated -10 dB impedance bandwidth can reach 2.87 GHz from 2.16 to 2.38 GHz and 2.91–5.56 GHz with 72.3% overall relative bandwidth. The measured eigenfrequencies of the FOR and SOR are 3.50 GHz and 4.98 GHz. The lower ZOR eigenfrequency is 2.28 GHz. The return loss of the fabricated antenna is measured using an Agilent E8361A network analyzer. The measured -10 dB impedance bandwidth is 70.1% (2.15–2.43 GHz and 3.06–5.55 GHz). The antenna is 32 mm \times 32 mm, with an overall size of around $0.23\lambda \times 0.23\lambda$, where λ is the free-space wavelength of the lowest frequency of 2.16 GHz.

In order to further demonstrate the operation mechanism, Fig. 8 shows the current distributions on the Y-shaped patch, AIS and ground plane. Most of the surface currents flow on the Y-shaped

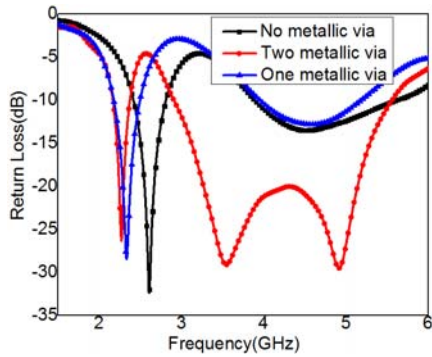


Figure 6. Simulated return loss of the proposed antenna with different numbers of the metallic shorting vias.

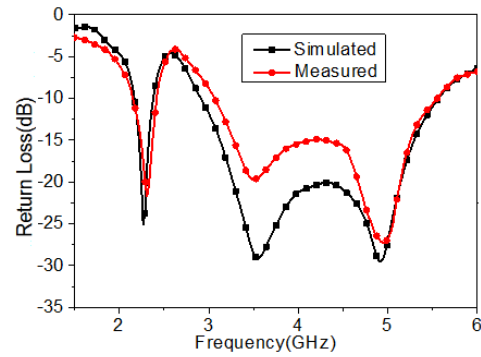


Figure 7. Simulated and measured return loss characteristics.

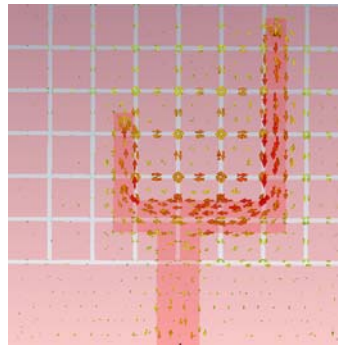


Figure 8. The current distributions on the ENG-TL antenna.

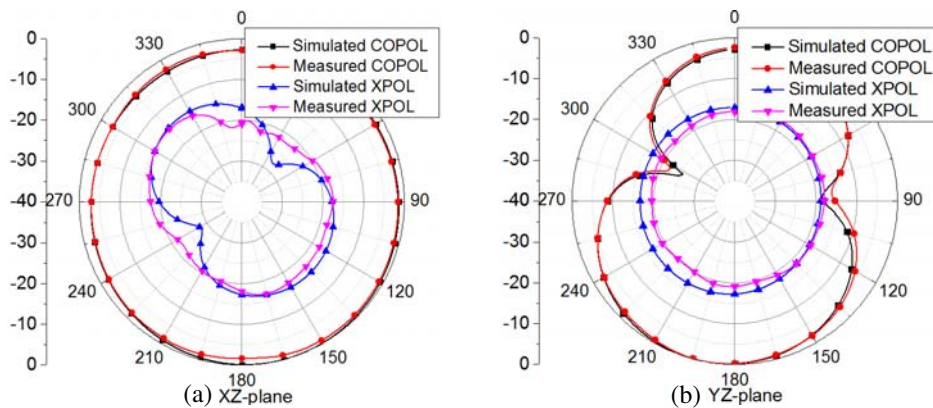


Figure 9. Simulated and measured radiation patterns of the antenna at 2.27 GHz. (a) XZ -plane, (b) YZ -plane.

patch, and part of the currents appear on the AIS. As a result, benefiting from the radiating gaps, the bandwidth of the ENG-TL antenna enhances.

The simulated and measured radiation patterns in two principal planes for the resonant frequency of 2.27 GHz are plotted in Fig. 9, and 3.5 GHz are plotted in Fig. 10. The results show that the radiation pattern in XZ -plane (E -plane) is approximately omnidirectional characteristic, and the radiation pattern in YZ -plane (H -plane) is monopole-like. The radiation energy is mainly focused in the Z -direction. Due to the asymmetric antenna structure, the gains of the cross polarization are

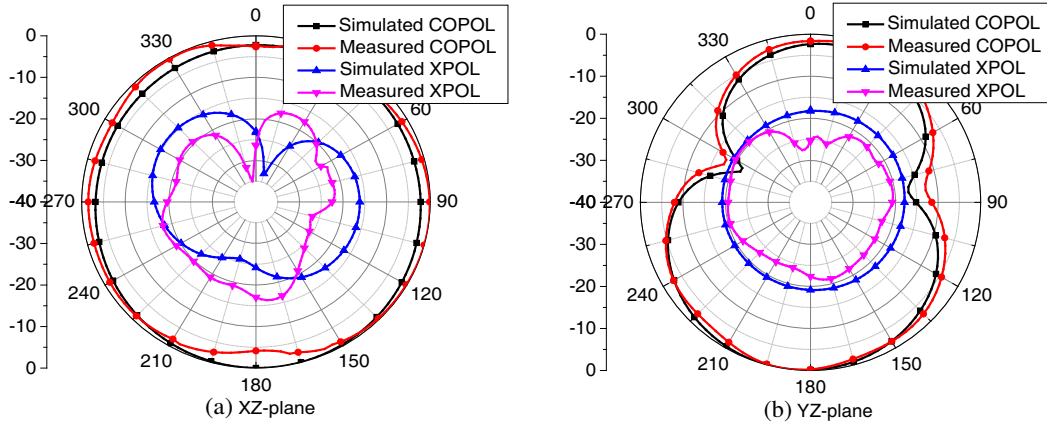


Figure 10. Simulated and measured radiation patterns of the antenna at 3.5 GHz. (a) XZ -plane, (b) YZ -plane.

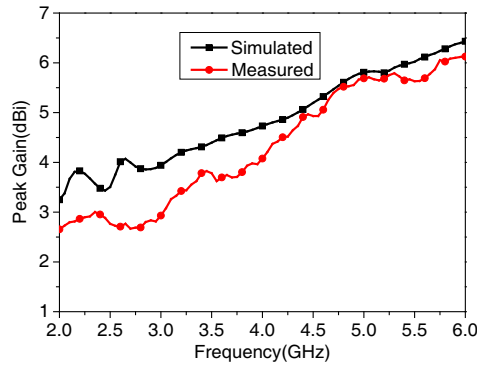


Figure 11. The measured and simulated peak gains of the ENG-TL antenna.

large in E -plane and H -plane.

As shown in Fig. 11, the simulated gains change from 3.22 dBi to 6.43 dBi. The discrepancy between simulated and measured gains could be attributed to fabrication process, soldering, and measurement environment. The measured radiation efficiency fluctuates from 73.2% to 81.3% over the band of 2.0–6.0 GHz. The proposed ENG-TL antenna simultaneously achieves wide bandwidth, high gain, and high radiation efficiency. The radiation pattern can satisfy application for broadband wireless communications.

5. CONCLUSION

A metamaterial-based broadband antenna employing optimized AIS has been proposed and demonstrated. The asymmetric Y-shaped patch connects to the ground plane by two metallic shorting vias. A novel artificial impedance substrate for antenna miniaturization with bandwidth extension technique is proposed. The fractional impedance bandwidth is 72.3%. The maximum gain is 6.43 dBi. The total size of the ENG-TL antenna is $0.23\lambda \times 0.23\lambda$. The antenna can be a good candidate for practical various wireless mobile communication systems.

ACKNOWLEDGMENT

This work was supported by the National Natural Science Foundation of China (Grant No. 61331007 and No. 61361166008), the Specialized Research Fund for the Doctoral Program of Higher Education of China (Grant No. 20120185130001), and the Project ITR1113.

REFERENCES

1. Wu, B.-I., W. Wang, J. Pacheco, X. Chen, T. M. Grzegorzcyk, and J. A. Kong, "A study of using metamaterials as antenna substrate to enhance gain," *Progress In Electromagnetics Research*, Vol. 51, No. 5, 295–328, 2005.
2. Jang, T., J. Choi, and S. Lim, "Compact coplanar waveguide (CPW)-fed zeroth-order resonant antennas with extended bandwidth and high efficiency on vialess single layer," *IEEE Trans. on Antennas Propagat.*, Vol. 59, No. 2, 363–372, 2011.
3. Herraiz-Martinez, F. J., V. Gonzalez-Posadas, L. E. Garcia-Munoz, and D. Segovia-Vargas, "Multifrequency and dual-mode patch antennas partially filled with left-handed structures," *IEEE Trans. on Antennas Propagat.*, Vol. 56, No. 8, 2527–2539, 2008.
4. Nordin, M. A. W., M. T. Islam, and N. Misran, "Design of a compact ultrawideband metamaterial antenna based on the modied split-ring resonator and capacitively loaded strips unit cell," *Progress In Electromagnetics Research*, Vol. 136, No. 1, 157–173, 2013.
5. Liu, W., Z. N. Chen, and X. M. Qing, "Metamaterial-based low-profile broadband mushroom antenna," *IEEE Trans. on Antennas Propagat.*, Vol. 62, No. 3, 1165–1172, 2014.
6. Huang, H., Y. Liu, S. S Zhang, and S. X. Gong, "Multiband metamaterial-loaded monopole antenna for WLAN/WiMAX applications," *IEEE Antennas Wireless Propag Lett.*, Vol. 14, No. 2, 662–665, 2015.
7. Bala, B. D., M. K. A. Rahim, and N. A. Murad, "A dual mode metamaterial antenna is proposed for wideband applications," *Microwave Optical Technol Lett.*, Vol. 56, No. 8, 1846–1850, 2014.
8. Bala, B. D., M. K. A. Rahim, and N. A. Murad, "Bandwidth enhancement metamaterial antenna based on transmission line approach," *Microwave Optical Technol Lett.*, Vol. 57, No. 1, 252–256, 2015.
9. Niu, B. J. and Q. Y. Feng, "Epsilon negative zeroth- and first-order resonant antennas with extended bandwidth and high efficiency," *IEEE Trans. on Antennas Propagat.*, Vol. 61, No. 12, 5878–5884, 2013.
10. Mosallaei, H. and K. Sarabandi, "Antenna miniaturization and bandwidth enhancement using a reactive impedance substrate," *IEEE Trans. on Antennas Propagat.*, Vol. 52 No. 9, 2403–2414, 2004.
11. Dong, Y. D., H. Toyao, and T. Itoh, "Compact circularly-polarized patch antenna loaded with metamaterials," *IEEE Trans. on Antennas Propagat.*, Vol. 59, No. 11, 4329–4333, 2011.
12. Dong, Y. D., H. Toyao, and T. Itoh, "Design and characterization of miniaturized patch antennas loaded with complementary split-ring resonators," *IEEE Trans. on Antennas Propagat.*, Vol. 60, No. 2, 772–785, 2012.
13. Xu, H. X., G. M. Wang, J. G. Liang, M. Q. Qi, and X. Gao, "Compact circularly polarized antennas combining meta-surfaces and strong space-filling meta-resonators," *IEEE Trans. on Antennas Propagat.*, Vol. 61, No. 7, 3442–3450, 2013.
14. Itoh, A., Lai, T. and C. Caloz, "Composite right/left-handed transmission line metamaterials," *IEEE Microwave Magazine*, Vol. 5, No. 3, 34–50, 2004.
15. Park, J. H., Y. H. Ryu, J. G. Lee, and J. H. Lee, "Epsilon negative zeroth-order resonator antenna," *IEEE Trans. on Antennas Propagat.*, Vol. 55, No. 12, 3710–3712, 2007.